



Research Article

Experimental investigation of impact of fire size on heat transfer and flame behavior of initial stage unsteady pool fires inside a cubical enclosure

Akanksha MATHUR^{1,2,*} , Anjan RAY¹ , S R KALE¹ 

¹Department of Mechanical Engineering, Indian Institute of Technology Delhi, New Delhi, 11016, India

²Department of Mechanical Engineering, The Northcap University, Sector 23A, Gurugram, 122107, India

ARTICLE INFO

Article history

Received: 24 April 2022

Accepted: 01 November 2022

Keywords:

Unsteady Growing Pool Fire; Heat Flux; Flame Behavior; Mass Loss Rate; Enclosure; Ceiling Duct

ABSTRACT

The ventilation equipment for enclosed spaces or office rooms is specified according National Building Code of India published by the Bureau of Indian Standards. Natural ventilation periodically together with mechanical ventilation is recommended to remove pollutants. The need to study fire and smoke behavior inside a completely closed room with air intake and exhaust vents becomes important in case of low or no mechanical ventilation service. An experimental study on unsteady heptane pool fires of different sizes in their initial stages was conducted in a cubical fire test chamber of 27 m³ inside dimensions. The compartment was naturally ventilated with a typical configuration of a vertical intake on a side wall and an exhaust vent at the ceiling leading into a duct. Three circular pans of diameters 0.34, 0.47 and 0.61 m were employed to generate the fire with n-heptane as fuel on a bed of water. Temperatures, wall heat fluxes and mass loss rate were measured. The flame was visualized using a video camera through a tempered view glass. The total heat transfer to the ceiling and wall increased with the increase in fire size as the flames became taller in the initial stages (3-4 minutes) with significant increase in case of 500 kW fire. The smoke layer was observed at about mid height (1.5 m) above floor. The leaning behavior of flames was seen due to naturally induced air inflow. The wall heat flux of about 50 kW/m² obtained indicate hazardous environment for further flame spread. A fourfold increase in mass loss rate was observed with just 2.5 times increase in fire size inside the ceiling vented compartment.

Cite this article as: Mathur A, Ray A, Kale SR. Experimental investigation of impact of fire size on heat transfer and flame behavior of initial stage unsteady pool fires inside a cubical enclosure. J Ther Eng 2023;9(6):1478–1489.

INTRODUCTION

Spills of liquid fuels and even molten thermoplastic materials in industrial settings, ship engine rooms, transport

industry and power plants pose a serious fire hazard. Some liquids are highly volatile which evaporate forming a flammable mixture with air that can subsequently cause an explosion in a confined space. Steady burning results in

*Corresponding author.

*E-mail address: akankshamathur@ncuindia.edu

This paper was recommended for publication in revised form by Regional Editor Zerrin Sert



a pool fire with a buoyant diffusion flame. Depending on the location, the fire could be a free burn/open pool fire that has no confining surfaces in the vicinity, or it could be a pool fire which is confined inside an enclosure, with or without openings. Open pool fires with simple geometry have been widely investigated [1-4]. The amount and type of combustible material is one of the main factors that influence the development of the fire [5-7]. A fuel package of a large surface area will burn more rapidly than an otherwise equivalent fuel package with a small surface area [5]. As the fuel size increases, the burning rate, the peak heat release rate (HRR) and flame height increase with accompanying increase in peak gas temperature and CO concentration inside reduced scale enclosures and ISO 9705 Room [8-10]. A pool fire burning rate is controlled by the heat transfer to the pool [11].

When the pool fire is enclosed, the behavior and structure of such a fire alters because of thermal feedback and interaction of plume with the surrounding walls, ceiling at different heights and constraints on ventilation [12]. A compartment fire has many parameters, including fuel type, heat release rate, burner location, nature of ventilation. The varying ventilation conditions greatly influence the characteristics of burning in terms of mass loss rate, temperature of ceiling and enclosure walls and gaseous species concentration [13-21].

Different studies have investigated a particular set of combinations because of the complex nature of the fires. Even the measured parameters and locations where the measurements were made are diverse. Limited knowledge is available on thermal aspects of a pool fire in a room or compartment with low intake of air and ceiling exhaust of gases through ducting. The results of compartment effects on such design fires will be helpful in safer design and fabrication of room interiors as durability of wall materials is affected by fire exposures [22]. The investigation of

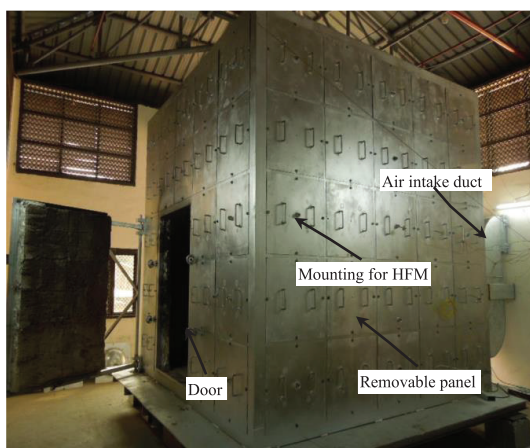
compartment fire with specific ventilation configurations is of great importance, because it provides data that concern building services.

This research includes design and fabrication of a test compartment of room size with ventilation through ducts and instrumentation of the compartment. This is followed by an experimental investigation of heptane pool fires in it with respect to the different fire sizes for the initial period of fire that occur before stationary stage, i.e. steady period of burning. The data reported can be helpful for simulations of such ceiling and wall vented compartment fires.

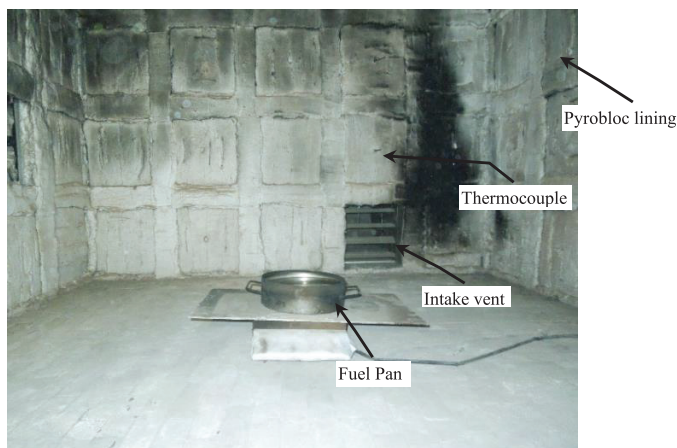
Experimental Setup

A fire test facility was designed and constructed which houses the fire test chamber (FTC) and instrumentation room. The photographs of the chamber exterior and interior are shown in Figures 1(a) and (b), respectively. Its internal dimensions are 3 x 3 m floor x 3 m height. The floor is made of a steel plate lined with refractory bricks. The walls and ceiling are made by assembling interchangeable panels (500 x 500 mm) held in place on a C-channel steel frame skeleton. One side of FTC has an access door. The inside of the frames and panels are lined with 150 mm thick Pyrobloc (high temperature insulation) lining. Some panels have openings for fitting thermocouples and heat flux sensors. One panel has a tempered glass window against which a visual camera is placed for videography of flames. One side wall panel was removed creating an intake vent and the opening was connected to an intake duct equipped with a damper. A ceiling panel was removed and connected to a chimney that led the smoke to the facility exterior.

Temperatures were measured with K-type thermocouples placed flush with wall inside or on the ceiling. In the temperatures reported in the results below, the radiation correction has not been applied. A weighing balance was used to measure the mass of the pan, water and fuel. The balance and its cable were fire resistant. To protect the



(a) Chamber exterior.



(b) Chamber interior.

Figure 1. Photographs showing the fire test chamber (a) interior and (b) exterior.

balance platform from the fire an asbestos sheet was placed on it. The range of the balance was 10 g to 50 kg with a resolution of 0.5 g. A Sony handy cam HDR-CX130 model was used to videograph the fire. It was mounted on a tripod stand in front of a removable panel with a tempered view glass.

Total heat flux was measured with air cooled heat flux sensor on a side wall. It is a heat flux micro sensor (HFM 6D/H) of Vatell make. It has a thermopile that occupies most of the surface area on the sensor face to measure heat flux. The device measures radiation and convection equally well with a 180° field-of-view. Its minimum detectable heat flux is 0.25 W/cm², calibration accuracy of $\pm 3\%$ and time response 300 μ s. The output of the sensor is connected to a differential amplifier (Vatell AMP-6) which gives a full scale ± 6 V output which is input to the DAS through BNC cable. A water cooled heat flux micro sensor (Vatell model HFM 1000-1), was installed on the ceiling. The outer body has two tubes for water inlet and outlet for water cooling. To minimize conduction from ceiling surface to the water cooled body, ceramic powder was filled inside the tube mounting specially fabricated for these sensors. The heat flux data was captured using NI PXIe 6341X series DAQ via 16-Single ended shielded BNC connector block. These instruments were connected to the data acquisition system (DAS). The uncertainty analysis of the instruments used in the experiments is presented in Table 1.

MATERIALS AND METHODS

A pool fire was produced by burning n-heptane in a circular pan. The damper connected to the intake duct and the ceiling vent was kept open. A series of experiments were conducted with three pan sizes placed at this room centre location. The pan size used were 340 mm, 470 mm and 610 mm in line with other studies conducted as documented in literature, see Table 2 below. The arrangement of instruments for this pan location is shown in Figure 2. After igniting the fuel using pilot ignition, the access door was closed. Some of the experiments were repeated and good repeatability was observed in most measurements. Each test has been designated with digits denoting ideal fire size according to pan diameter, and two letters denoting fire location.

RESULTS AND DISCUSSION

Multiple experiments for each pan size were performed. Table 3 shows the test matrix of the experiments conducted inside FTC. Variations in measurement of temperatures and heat flux with central pool fire cases are discussed below. Flame behavior observed is also detailed.

Measurement of Temperature

Figure 3 shows ceiling temperatures at four locations for all the three pans. Location of TC3c, (in Figure 3 (a)) is above the pan, and other locations are as per Figure 2.

Table 1. Uncertainty of measurement by instruments used

Instrument	Component Standard Uncertainty	Combined Standard Uncertainty
Temperature (Omega make K-type thermocouple)		
Calibration of thermocouple with extension wire	$\pm 1.6\%$ ($\pm 12.8\text{ }^\circ\text{C}$)	-11 % to +3.4%
Radiative cooling	(-10.5 % to 0 %)	
Random	$\pm 3\%$	
Heat Flux (Vatell model heat flux micro sensor)		
Soot Deposition	$\pm 10\%$	12%
Cooling Water Temperature	$\pm 5\%$	
Calibration	$\pm 3\%$	
Random	$\pm 3\%$	

Table 2. Test matrix data from existing literature

Pan conditions	Reference no.
0.3m x 0.3m and 0.5m x 0.5m square steel pans (with a 2 mm thickness) with pan height was 3 cm and 5 cm, Heptane pool fire, 70 m ³ setup	[23]
10, 15, 20, 30, and 35 cm diameter pans, engine room dimension -3 m (l) x 3 m (w) x 3.5 m (h), n heptane pool fires	[24]
Pool diameters of 0.3, 0.5, 0.7 and 1.0 m (with 2 mm thick) gasoline, open pool fires	[25]

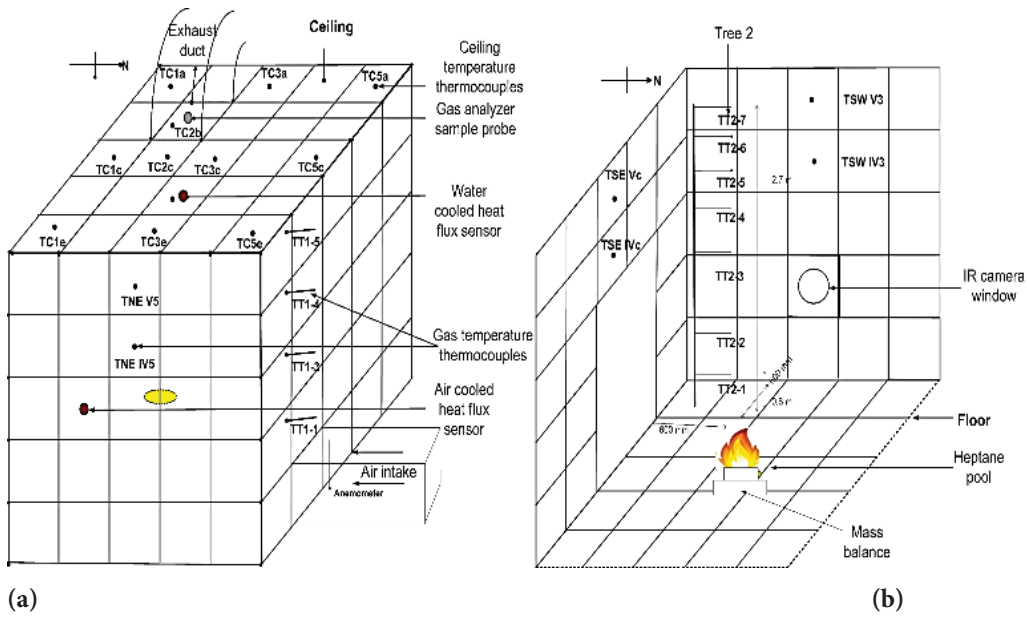


Figure 2. Schematic diagram of the instrument location in the chamber for room centre fire configuration. (a) Showing NE, Ceiling and NW side walls and (b) showing floor, SE and SW walls.

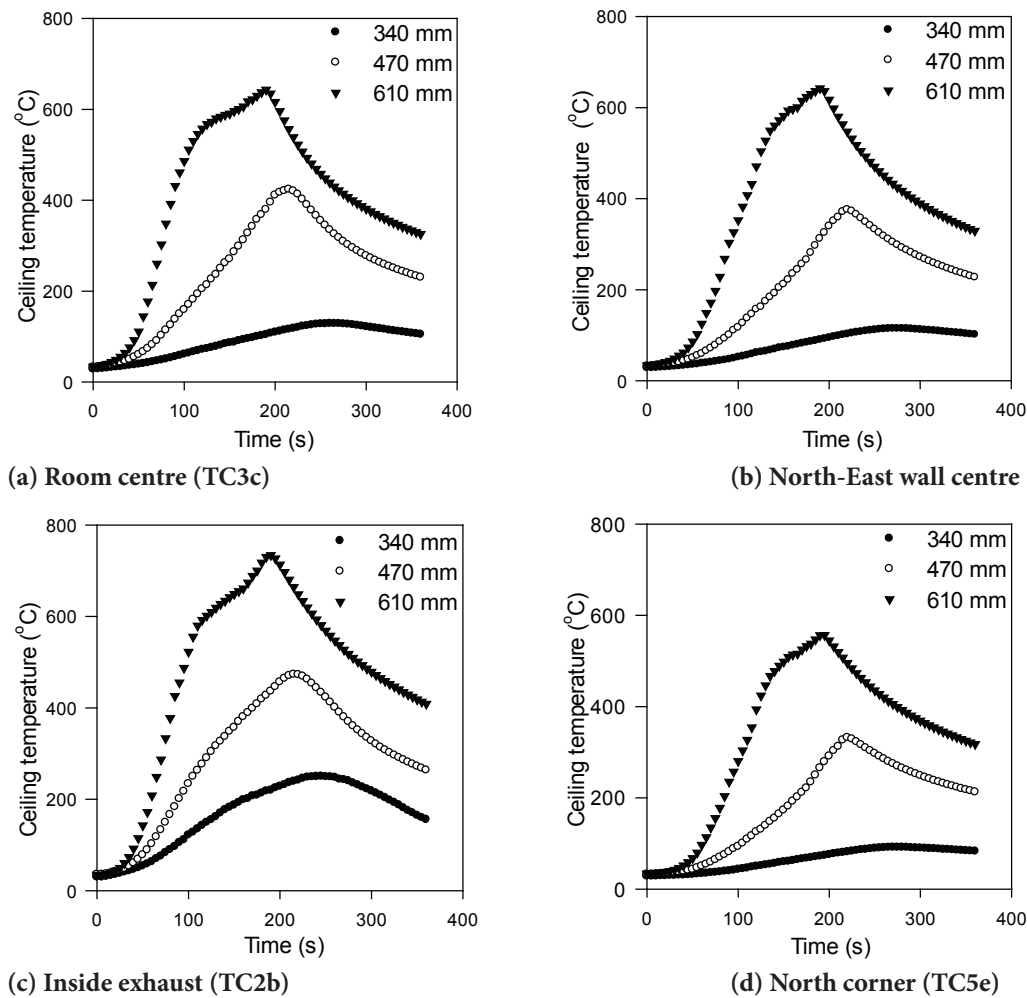


Figure 3. Temporal variations of ceiling temperatures at different locations (a) centre of room ceiling (b) centre of the north east side wall (c) inside exhaust duct in the plane of ceiling and (d) north corner of room ceiling.

Table 3. Test matrix of the experiments conducted inside FTC

Test no.	Pan. dia.	Nominal fire size (kW)	Pan location	Pan center location		No. of experiments.
	(mm)			X (m)	Z (m)	
100 RC	340	100	Centre	1.5	1.5	06
250 RC	470	250	Centre	1.5	1.5	03
500 RC	610	500	Center	1.5	1.5	01

TC2b is close to the ceiling vent. The flow of smoke towards the vent and the opposite location of the intake cause the fire to tilt and impinge away from the ceiling center. Thus, the locations TC3e and TC5e close to the north corner had temperatures less than those at the center. These temperatures were higher for 470 mm pan size than 340 mm due to taller flames and hotter ceiling jet plumes. In case of 610 mm pan diameter, TC3c and TC3e peak temperatures were same (i.e. 645 °C) because of the full involvement of room along with more entrainment and mixing after breaking of view glass.

Wall temperatures on three sides at two vertical locations of 2.1 m and 2.7 m above the floor are presented in Figure 5 for the three pan sizes. These heights respectively correspond to 0.9 and 0.3 m below the ceiling.

At the SE wall, Figure 4(a), temperatures at both heights are similar for 340 mm pan diameter fires. Temperatures for 340 and 470 mm diameter pans are similar with no discernable dependence on elevation. For the 610 mm diameter pan, near ceiling temperatures (at 2.7 m elevation) are lower than those below (at 2.1 m elevation). Because of oxygen starvation, consequently, the fire area expanded drastically and shifted nearer to the intake space. The view glass on the south east wall was damaged which caused rapid entrainment through the broken window and, hence, combustion increased near the south east wall at lower locations. This could not be recorded as the camera was damaged.

On the north east wall, Figure 4(b), for 340 mm pan the temperatures are lowest at less than about 150 °C. For 470 mm diameter pan, peak temperatures are about 480 °C and the 610 mm. diameter pan recorded temperatures as high as 725 °C. The south west wall temperatures are shown in 5 (c) where temperatures at 2.7 m and greater than those at 2.1 m elevation. In all figures, it can be seen that larger fires produce greater temperatures.

Figure 4 shows that larger pans cause steeper rise in temperatures and also higher peaks as observed in reported literature [24, 25]. At every location, the temperatures peaks just before extinction in initial fire growth stage. Amongst the walls, at either elevation, the highest temperatures occurred on the south east wall which is opposite to the intake opening. Increased dilution of fresh air and hot gases near the vents decreases away from them. Moreover, the flow induced from intake vent opening in room tilts the flame and plume towards southeast wall.

The larger the pan, the larger is the effect of enclosure on the pool fire. The flames increase in size (length) with the increasing pool diameter. The resulting longer flames and their taller plumes directly impinge on the ceiling, and quickly spread and descend in the form of smoke layer zone. Figure 5 shows gas temperature in a vertical line along a thermocouple tree near the exhaust for 340 and 470 mm diameter pans. A two layer temperature profile development is observed which suggests that a smoke layer is built up to 1.5 m above the floor. For the 470 mm pan the smoke layer builds up at 100 s which is faster than the smaller pan.

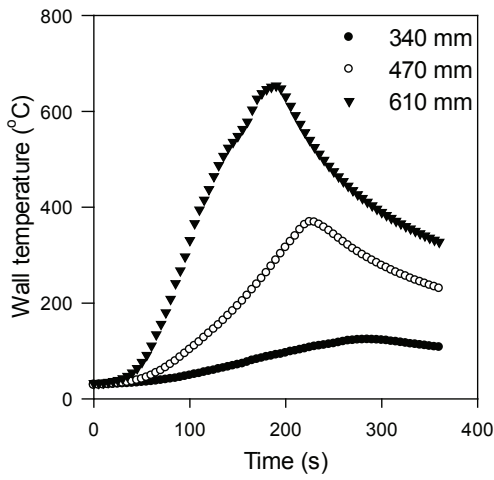
Isotherm Contours for Ceiling

Isotherm contours on the ceiling are shown in Figure 6 for three pan sizes 200 s after ignition. For 340 mm pan, highest temperatures (about 240 °C) occur around the ceiling vent. For the 470 mm diameter pan fire also, the highest temperatures occur near the ceiling vent, as in Figure 6(b). The ceiling temperatures with 470 mm pan size are around 200 °C greater than those with 340 mm pan size. At 200 s, in the former case the flame was nearing its peak but in latter case the fire was about to extinguish. This is cause for higher temperatures near the exhaust in 340 mm pool fire whereas effect of mixing can be seen in ceiling temperatures in the 470 mm pool fire case. Figure 6(c) shows the ceiling temperature contour at 200 s for largest pan (610 mm) size and temperatures above 800 °C are seen above intake and south east wall as the flame detached from pan and shifted towards oxygen rich zones at 200s.

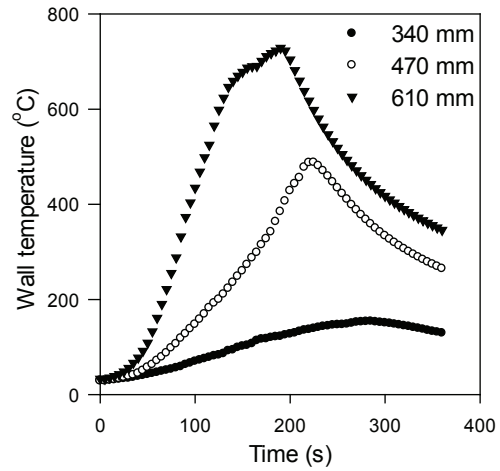
Measurement of Heat Flux

Figure 7(a) shows total heat flux variation with time on the ceiling panel adjacent to the panel vertically above pool fire centre, and Figure 7(b) shows the total heat flux on the NE wall at 1.5 m elevation. The ceiling heat flux increased five times for 470 mm compared to 340 mm and peak value was 50 kW/m². This is enough to ignite common combustible materials. The incident heat flux was about 10 kW/m² in 340 mm pool fire burning which heightened ten times in magnitude for 610 mm diameter pan to a value of 120 kW/m². Maximum and average values of ceiling heat flux for all tests are presented in Table 2.

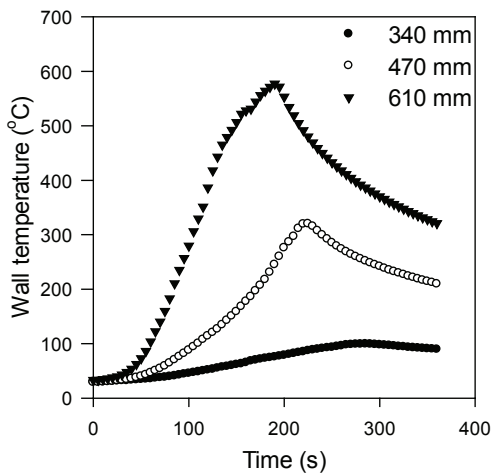
At mid-height above floor on the wall, the heat flux is smaller for the two smaller pans i.e., 340 mm and 470 mm about 11 and 35 kW/m² respectively. However, for the 610 mm pan, there is a sudden increase in heat flux after 150 s



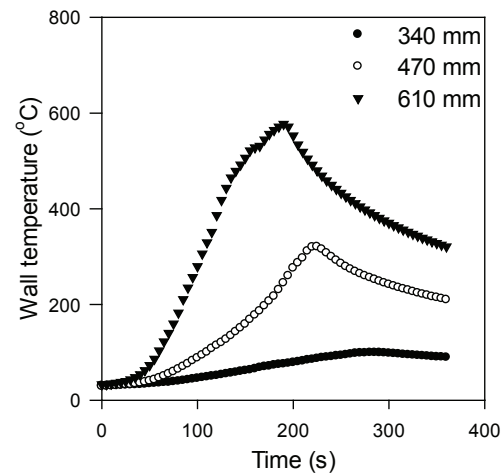
(i) 2.7 m elevation (TSE VC)
(a) South-East wall



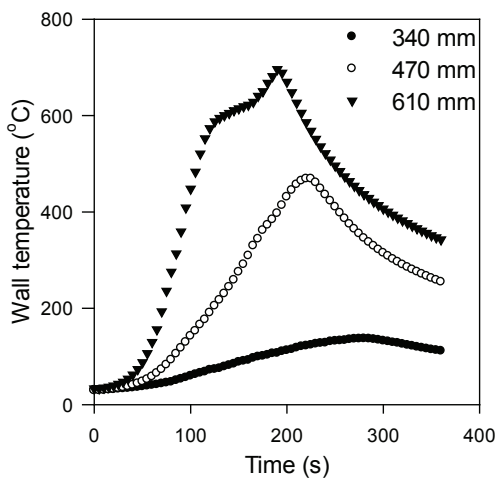
(ii) 2.1 m elevation (TSE IVC)



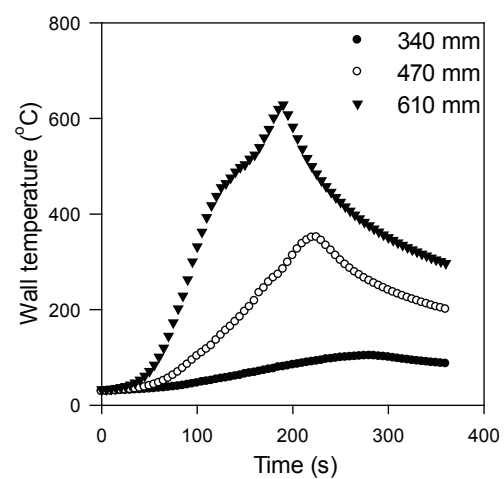
(i) 2.7 m elevation (TNE V3)
(b) North-East wall



(ii) 2.1 m elevation (TNE IV3)

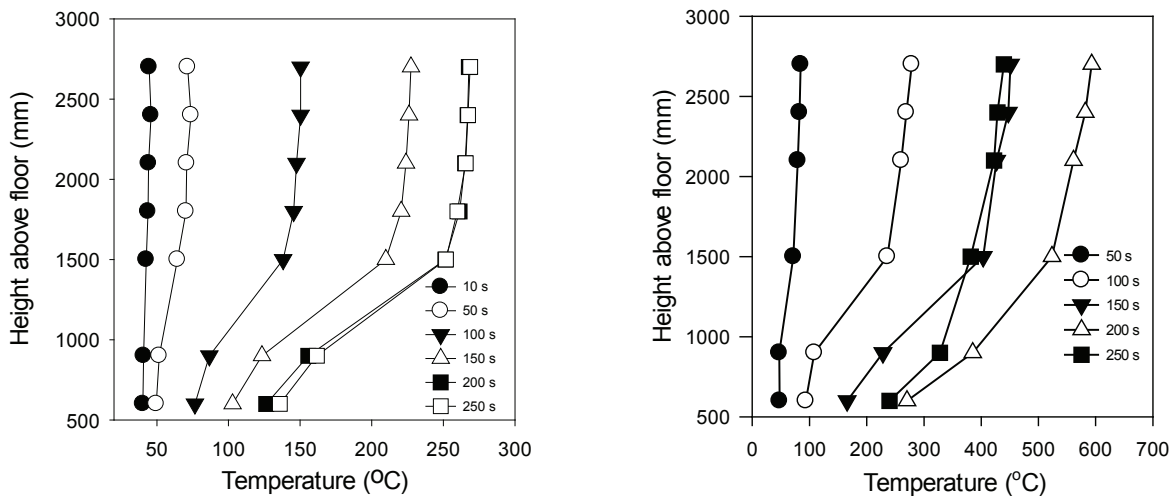


(i) 2.7 m elevation (TSW V3)
(c) South-West wall



(ii) 2.1 m elevation (TSW IV3)

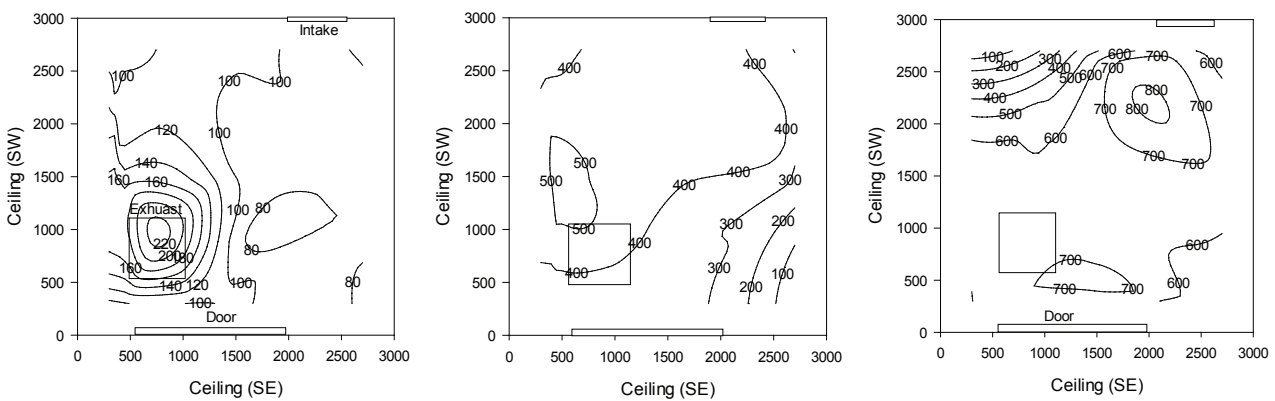
Figure 4. Variation of wall temperatures at (i) 2.7 m and (ii) 2.1 m above the floor on (a) South-East wall, (b) North-East wall, and (c) South-West wall for three pan sizes.



(a) 340 mm diameter pan.

(b) 470 mm diameter pan.

Figure 5. Vertical gas temperature profiles near the exhaust inside FTC for (a) 340 mm and (b) 470 mm pan diameter pool fires.

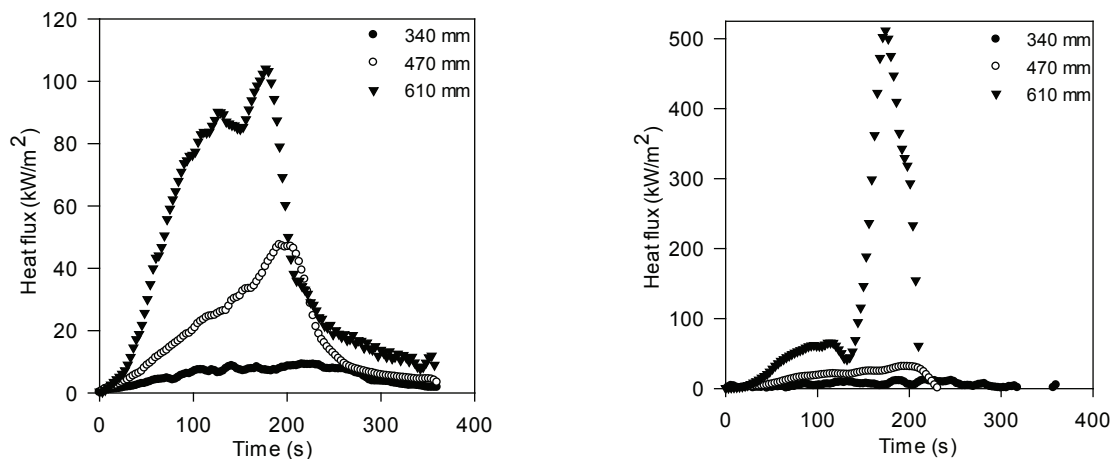


(a) 340 mm diameter pan.

(b) 470 mm diameter pan.

(c) 610 mm diameter pan.

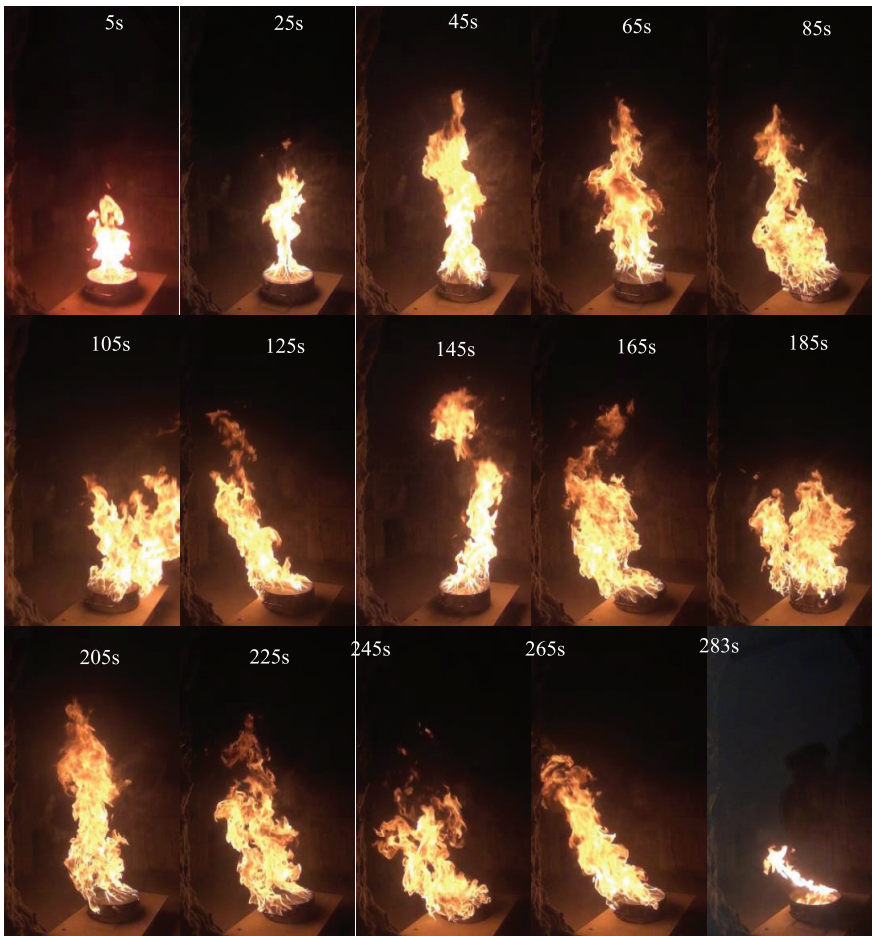
Figure 6. Ceiling temperature contours for (a) 340 mm, (b) 470 mm, and (c) 610 mm diameters pan fires at $t=200$ s after ignition.



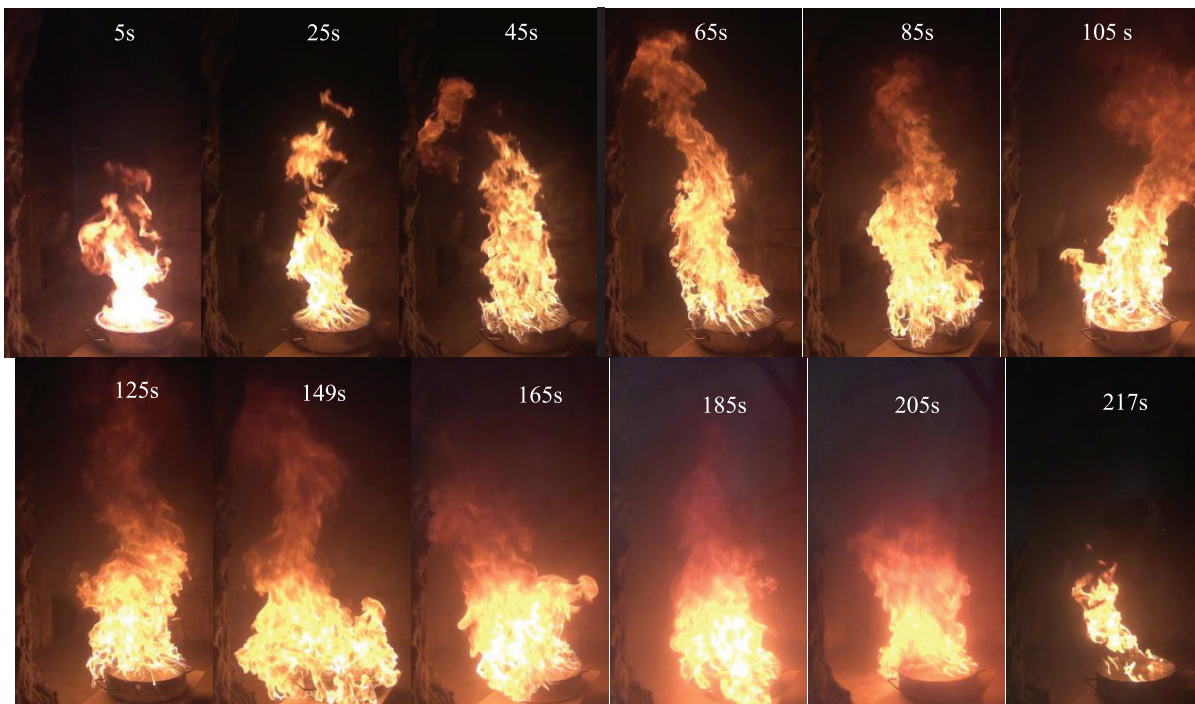
(a) Ceiling

(b) Wall

Figure 7. Variation of heat flux with time on (a) ceiling 0.84 m from the location vertically above the pool centre, and (b) north-East wall at 1.5 m above floor.



(a) Sequence of pool fire for 340 mm diameter pan at different time instants from $t = 5$ s to 283 s after ignition.



(b) Image sequence of pool fire for 470mm pan diameter at different time instants from $t = 5$ s to 217 s after ignition.

Figure 8. Photographs of transition of *n*- heptane pool fire placed centrally in fire test chamber from ignition to extinction.

of burning. Significantly large heat flux of about 500 kW/m² is seen on the wall. This value is much more than seen in a typical flashover environment. This heat flux on the wall is nearly 5 times that on the ceiling; this phenomenon can be explained by the flame spread in the chamber both vertically and horizontally. Similar effects were observed in past studies [19].

The bigger pan size (500kW) had significant enhancement in the flame height and area and hence, the heat transfer in form of convection and radiation to the surroundings and ceiling. During the experiment videography was stopped due to damage to the view glass. Also at the ceiling, the slope of the total heat flux variation is more for larger pan size of 610 mm as compared to 470 mm.

Experimental Study on Flame Behavior

Figure 8(a) presents the sequence of flame pictures from the video for 340 mm pan fire. For the first 25 s, the flame is straight and then gradually starts tilting towards south after 65 s which later becomes unstable. Tilting is due to air flow for combustion from intake which exits from the exhaust vent. While remaining attached to the top of the fuel pan, the flame expands horizontally beyond the lip of the pan in a random manner and at no discernable rate. After expanding, the flame base drops on the sides of pan. The flame also swirls in between; a tilt on the opposite side was visible around 55 s, again after 70 s at 125 s and then, after 60–70 s at about 195 s. The flames after swirl motion returned back to its original tilt in the exhaust direction. The fire decays after 265 s and was extinct at 283 s.

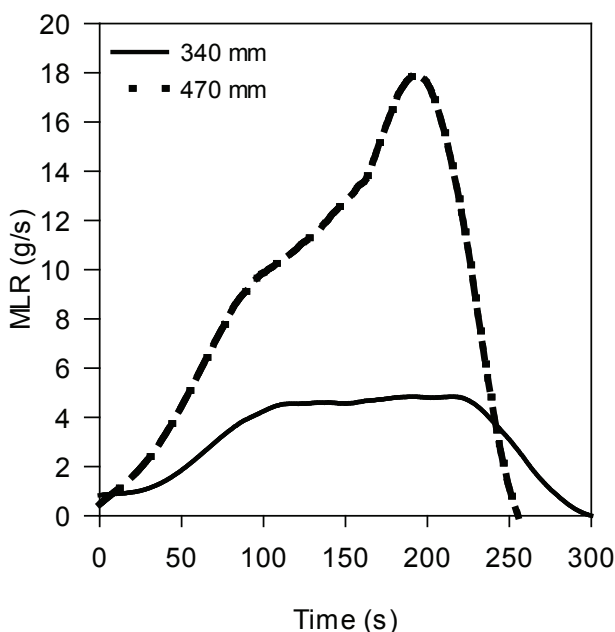


Figure 9. Time evolution of average mass loss rate for 340 and 470 mm pan sizes in room centre fires.

The flames were elongated as seen in Figure 8 (b) showing sequence of images for 470 mm pan diameter fire. The flame shape, length and area increased with the pan size. The flames increased in length quickly up to 45 s then the flame length was nearly maximum and tilting starts. The expansion of area of flames begins; it has enhanced from 340 mm pan to 470 mm pan case. And hence, the heat transfer from flames to walls and ceiling increased. The irregular dropping beyond edges of pan is also more frequent. At 149 s, the flaming zone expansion beyond and below pan was maximum. The flame also detached from the fuel surface. The swirl phenomenon was not noticeable because of this large and irregular expansion. The fire decay starts after 185 s till extinction around 217 s. As oxygen gets consumed faster for the larger fires, there is beginning of under ventilation condition; the flames become less luminous for 470 mm pan size.

The flame visualization of 670 mm pan was incomplete because of the breaking of view glass during fire experiment. A similar flame behavior, termed as “expanding flames,” has been seen [26] in under ventilated conditions for steady state fires. In the present study, such phenomenon was seen observed in the case of 340 and 470 mm pool fires for initial fire growth stage inside the FTC.

Measurement of Mass Loss Rate

Peak mass loss rate enhanced 4 times i.e., from 5 g/s for 340 mm pan to 20 g/s for 470 mm pan, Figure 9. Maximum and average values of mass loss rate for all tests are listed in Table 3.

The slope of mass loss rate is also steeper for the larger pan in the short duration initial stage fires in line with existing literature [12]. The fire starts decaying at about $t = 235$ s and 200 s after ignition for the former and latter case respectively. As the fuel gets consumed, the fire decays (in size) which in turn decreases thermal feedback to the pool surface. The fuel evaporation rate drops until the fuel gets exhausted. During the experiment with 610 mm diameter pan, the mass loss data could not be recorded because the weighing balance instrument was badly damaged during this experiment.

Some simulations were carried out to understand the mass loss rate in open fire using Pyrosim software. Comparison of MLR was carried out between the open fire and room centre configuration which is presented in Fig 10. Initial conditions for the fire modeling are considered as the quiescent conditions inside the chamber and for the open space as well where initial velocity of air inside the enclosure is zero. The ambient temperature of 298 K and pressure of 101.5 kPa was considered. All the wall and surface had initial temperatures as that of ambient temperature. Relative humidity was taken to be 50 %. The chamber domain is modeled as per the actual experimental set up. The mass loss rate immediately peaked to the 2.4 g/s and became steady at this value. In case of room centre configuration, peak value was approached gradually during 120 s.

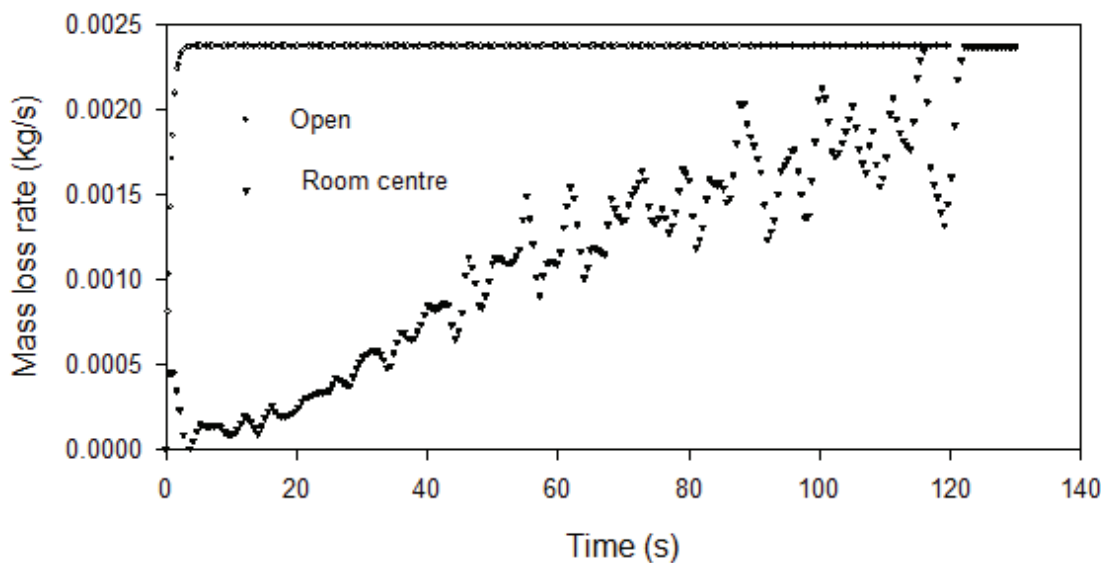


Figure 10. Temporal variation of mass loss rate predicted by CFD for – open pool fire and room centre configuration inside fire test chamber.

Table 4. Mass loss rate and Ceiling heat flux of the different tests

Pan size (mm)	Mass loss rate (g/s)		Heat flux at ceiling	
	Max	Mean	Max	Mean
340	5	4.7	13	10.1
470	19.8	18.1	50	47.4

This behavior shows that mass loss rate gradually increases as natural air flow establishes through the intake opening which does not happen in case of quiescent atmosphere as indicated in past studies [27].

RESULTS AND DISCUSSION

Generally, a two zone vertical temperature profile was seen for room centre experiments, indicating impact of compartment walls. Total heat flux on ceiling and side wall increased with the increase in pool surface area for the initial stage transient pool fires. As the flame area increases, the resultant convection and radiation to the walls also increase. As the pan size increases, the enclosure effects are more pronounced in this short duration of 3-4 minutes.

The mass burning rate increases substantially as does the total heat flux on the ceiling and the wall and, hence, indicate they are functions of the size of the fire for initial fire ignition and growth part in this pool fire study inside a typical ceiling ducted environment. Similar observations are reported in literature [29].

The flame height was computed from images digitalized from the video recordings using MATLAB. Flame height for 340 mm pan diameter increases for about 100 s and then

fluctuates around an average of 1.1 m from about 100 to 260 s before decaying. The height was about 200 mm more for the 470 mm pan fire in the initial 50 s, but after that the flame-lets frequently reached beyond the field of view and only the luminous flame was detected because of smoke layer descending down. The larger fire resulted in taller flames which directly impinge on the ceiling thereby rapidly increasing compartment temperatures. Thermal feedback from ceiling zone to the fuel upper surface enhances fuel evaporation rate. Analysis of the videos showed that for room centre fires, the flame initially is straight with oscillatory (puffing) behavior and after some time it gradually starts tilting south-wards, i.e. in the direction of the exhaust vent. Subsequently, the flame extends beyond the sides of the pan and swirls periodically, returning back to its tilted position. The tendency of flames to tilt towards the exhaust was due to the low velocity air flow induced from the intake vent. Similar trend was reported in the literature [27, 28] for open and enclosure pool fires.

CONCLUSION

In the present work, the initial transitory stage of fire growth for medium scale pool fires in a compartment is

carried out. Temperatures, mass loss rate and heat flux were measured for n-heptane pool for the beginning phase of fire within 3 minutes inside the enclosed chamber. The major conclusions for the work presented are as follows.

- The trends in temperature show that as pan size increases, the enclosure effects are more pronounced. This was majorly because of the increased heat feedback to flame surfaces even in initial 2-3 minutes of unsteady fire growth.
- The experimental results revealed that large pan pool fires have 18-20% taller flames and plumes. As a result, the smoke layer builds faster for larger pools. Consequently, an increase in the compartment temperatures for larger pool fires is seen. A rapid rise in ceiling temperatures at rate of 2.15 times is seen w.r.t pool size.
- The heat flux incident on wall and ceiling of the chamber are functions of pool size during the initial phase after ignition. Such unsteady pool fires of 100, 250 and 500 KW, studied in this work resembled typical size of common fire sources in real fire scenarios inside vented spaces. Several common combustible wall or interior decorative materials will be ignited as the maximum heat fluxes observed were above 50 KW/m².
- In the present study, an air in flow was induced through vent which tilted/leaned the flames in its path. Flame geometry was affected by the presence of vents and their location.
- The increase in mass loss rate with pan diameter by nearly 4 times was marked for initial stage fire in naturally vented fire configuration with lower intake and ceiling exhaust.
- During the initial stage unsteady fire experiments, oxygen starvation expanded the flames beyond and below the fuel pan sides.

ACKNOWLEDGMENTS

This work was performed under a project funded by Bhabha Atomic Research Centre, Mumbai. Their support is gratefully acknowledged. Declarations of interest: none.

AUTHORSHIP CONTRIBUTIONS

Authors equally contributed to this work.

DATA AVAILABILITY STATEMENT

The authors confirm that the data that supports the findings of this study are available within the article. Raw data that support the finding of this study are available from the corresponding author, upon reasonable request.

CONFLICT OF INTEREST

The author declared no potential conflicts of interest with respect to the research, authorship, and/or publication of this article.

ETHICS

There are no ethical issues with the publication of this manuscript.

REFERENCES

- [1] Hamins A, Kashiwagi T, Buch RR. Characteristics of pool fire burning. ASTM Spec Tech Pub 1996;1284:15–41. [\[CrossRef\]](#)
- [2] Babrauskas V. Free burning fires. Fire Safe J 1986;11:33–51. [\[CrossRef\]](#)
- [3] Joulain P. The behavior of pool fires: state of the art and new insights. Symp Comb Proc 1998;27:2691–2706. [\[CrossRef\]](#)
- [4] Quintiere JG. Fire behavior in building compartments. Proc Comb Inst 2002;29:181–193. [\[CrossRef\]](#)
- [5] Drysdale D. An introduction to fire dynamics. 3rd ed. England: John Wiley & Sons; 2011. [\[CrossRef\]](#)
- [6] Mathur A, Vikas DH, Kale SR. An Experimental Study on Burning of Vertical Cloth Panels. Fire Saf Sci 2011;10:485–498. [\[CrossRef\]](#)
- [7] Babrauskas V. Estimating large pool fire burning rates. Fire Technol, 1983;19:251–261. [\[CrossRef\]](#)
- [8] Bundy MF, Hamins AP, Johnsson EL, Kim SC, Ko G, Lenhart DB. Measurements of heat and combustion products in reduced-scale ventilation-limited compartment fires. Tech Note (NIST TN); Gaithersburg: Natl Inst Stand Technol; 2007. [\[CrossRef\]](#)
- [9] Lock A, Bundy M, Johnsson EL, Hamins A, Ko GH, Hwang CH, et al. Experimental study of the effects of fuel type, fuel distribution, and vent size on full-scale under ventilated compartment fires in an ISO 9705 room. Tech Note (NIST TN); Gaithersburg: Natl Inst Stand Technol; 2008. [\[CrossRef\]](#)
- [10] WK C, WL C. Experimental studies on forced-ventilated fires. Fire Sci Technol 1993;13:71–87. [\[CrossRef\]](#)
- [11] Babrauskas V. Heat release rates. In: Hurley MJ editor. SFPE Handbook of Fire Protection Engineering. 5th ed. New York; Springer: 2016. p.799–904. [\[CrossRef\]](#)
- [12] Liu J, Chen M, Lin X, Yuen R, Wang J. Impacts of ceiling height on the combustion behaviors of pool fires beneath a ceiling. J Therm Anal Calorim 2016;126:881–889. [\[CrossRef\]](#)
- [13] Andrews GE, Ledger J, Phylaktou HN. Pool fires in a low ventilation enclosure. Inst Chem Eng Symp Ser; UK: Inst Chem Eng; 2000. p. 171–184.
- [14] Pretrel H, Suard S, Audouin L. Experimental and numerical study of low frequency oscillatory behaviour of a large-scale hydrocarbon pool fire in a mechanically ventilated compartment. Fire Saf J 2016;83:38–53. [\[CrossRef\]](#)
- [15] Mense M, Pizzo Y, Pretrel H, Loraud JC, Porterie B. Experimental parametric study on low-frequency oscillating behaviour of pool fires in a small-scale mechanically-ventilated compartment. Journal of Physics: Conference Series: IOP Publishing; 2018. [\[CrossRef\]](#)

- [16] Mense M, Pizzo Y, Pr  treel H, Lallemand C, Porterie B. Experimental and numerical study on low-frequency oscillating behaviour of liquid pool fires in a small-scale mechanically-ventilated compartment. *Fire Saf J* 2019;108:102824. [\[CrossRef\]](#)
- [17] Zhang S, Ni X, Zhao M, Zhang R, Zhang H. Experimental study on the characteristics of wood crib fire in a confined space with different ventilation conditions. *J Therm Anal Calorim* 2015;120:1383–1391. [\[CrossRef\]](#)
- [18] Babrauskas V. Estimating room flashover potential. *Fire Technol* 1980;16:94–103. [\[CrossRef\]](#)
- [19] Liu Q, Ma Q, Zhang H, Yang R, Wei D, Lin CH. Experimental study on n-heptane pool fire behavior under dynamic pressure in an altitude chamber. *J Therm Anal Calorim* 2017;128:1151–1163. [\[CrossRef\]](#)
- [20] Chandra AS, Reddy PN, Harish R. Natural ventilation in a lege space with heat source: CFD visualization and taguchi optimization. *J Therm Eng* 2022;8:642–655. [\[CrossRef\]](#)
- [21] Sereir T, Missoum A, Mebarki B, Elmir M, Douha M. Effect of the position of the hot source on mixed convection in a rectangular cavity. *J Therm Eng* 2021;8:538–550. [\[CrossRef\]](#)
- [22] Karbhari VM. Introduction: the use of composites in civil structural applications. *Durability of composites for civil structural applications*. 1st ed. Woodhead Publishing: 2007. p. 1–10. [\[CrossRef\]](#)
- [23] Brohez S, Saladino D, Perelli M, Experimental and Numerical Study of Heptane Pool Fire. *Chem Eng Trans* 2022,91:223–228.
- [24] Wang J, Jiao Y, Shi L, Xie Q, Li G, Liu J, et al. An experimental and non-dimensional study on the vertical temperature distribution of a sealed ship engine room fire. *Ocean Eng* 2018;165:22–33. [\[CrossRef\]](#)
- [25] Sudheer S, Saumil D, Prabhu SV. Physical experiments and Fire Dynamics Simulator simulations on gasoline pool fires. *J Fire Sci* 2013;31:309–329. [\[CrossRef\]](#)
- [26] Loo AX, Coppalle A, Yon J, A  n   P. Time-dependent smoke yield and mass loss of pool fires in a reduced-scale mechanically ventilated compartment. *Fire Saf J* 2016;81:32–43. [\[CrossRef\]](#)
- [27] Jiang P, Lu SX. Pool fire mass burning rate and flame tilt angle under crosswind in open space. *Procedia Eng* 2016;135:261–274. [\[CrossRef\]](#)
- [28] Woods JA, Fleck BA, Kostiuik LW. Effects of transverse air flow on burning rates of rectangular methanol pool fires. *Combust Flame* 2006;146:379–390. [\[CrossRef\]](#)
- [29] Delichatsios MA, Silcock GW. Fully involved enclosure fires: effects of fuel type, fuel area and geometry. *Fire Saf Sci* 2003;7:59. [\[CrossRef\]](#)